# Nozzle and Working-Condition Classifications for Water Jet Systems

Massimo Lazzaroni, *Member, IEEE*, Stefano Ferrari, *Member, IEEE*, Loredana Cristaldi, *Senior Member, IEEE*, and Massimiliano Annoni

***Abstract*—In this paper, a technique for assessing both the working and healthy conditions of water jet-system nozzles is presented. The proposed classifier is based on the discrete Fourier transform (DFT) of the instantaneous electrical power signal. With this in mind, it will be shown that the electrical power signal supports all necessary information to characterize both the working condition of the system and the nozzle type. Furthermore, the same signal can be analyzed with the aim of predicting the presence of an incoming faulty behavior. The presented technique is also used to build a second type of classifier. While the first one is of general application, the second one can be used when the properties of the orifice are known, and only the working conditions have to be classified. Results show the effectiveness of the proposed approach, which, due to its simplicity, can be embedded in a low-cost real-time diagnostic system. For the sake of clarity, a brief description of a water jet system is also presented.**

***Index Terms*—Fault diagnosis, feature extraction, pattern classification, pattern recognition (PR), power measurement, statistical process control, water jet systems.**

## I. Introduction

WATER JET and abrasive-WJ (WJ/AWJ) technology is often used in application fields where particular manufacturing operations on special materials are required, such as cutting hard-to-machine materials or carrying out operations, such as turning and milling. In fact, the AWJ cutting process is a cold process as the water takes heat away from the interested area of the workpiece. In every situation where it is necessary to carry out an operation without damaging the metallic material structure of the piece being worked on, the aforementioned technology is very useful, and in many cases, its use is mandatory.

The efficiency of the WJ system is influenced by the status of the water nozzle. This component plays an important role in the definition of the efficiency, which is measured as the ratio between the available fluid-dynamic power and the electric active power from the network. Starting from this consideration, it would be noted that a monitoring activity devoted to evaluating the efficiency of the nozzle is mandatory to predict the efficiency of the AWJ system.

Starting from the simple consideration that the acquired electric signals give useful indications for diagnosis purposes [1], it is a little step to consider a continuous nonintrusive on-field monitoring activity during all the plant components' life.

It would be shown that different power consumptions lead to differences that are sometimes relatively large in terms of cutting performance as well as of the operating costs of the system. Furthermore, it is shown that it is possible to extract information on the behavior of the AWJ system from the power signal, and this could allow the detection and anticipation of incorrect operating conditions.

The aim of this paper is to set up a technique to extract information from the electrical power signal about the working condition of the system. In particular, the interest is focused in identifying both the nozzle type and its working condition by means of an ad hoc developed signature for each nozzle under each working condition, which allows the correct classification.

The collection of the power-signal samples for several nozzle types and working conditions allows us to build up a nozzle footprint database. Such a database constitutes the knowledge for the automatic recognition of the mounted nozzle and its working condition based on pattern-recognition (PR) techniques. In Section II, a brief description of a WJ/AWJ system has been presented, while in Section III, an introduction concerning PR has been presented. The classification tool is presented in Section IV, while Section V reports the experimental results. In Section VI, the results and peculiarities of the proposed approach are discussed. Conclusions follow in Section VII.

## II. Proposed System Architecture for Classification Purposes

The AWJ technology [1]–[12] exploits phenomena belonging to different fields of physics. Considering a complete WJ cutting system, shown in Fig. 1, electrical energy is provided at first to the 400-V, 50-Hz, three-phase induction motor that pressurizes the oil by means of the radial-piston oil pump.

The oil circuit pressure could reach a value of 20 MPa. The oil provides its hydraulic energy to water by means of the double-acting intensifier, increasing the water pressure up to 400 MPa. An accumulator reduces the water pressure fluctuations [1]–[6]. When water reaches the cutting head and flows through the orifice, the pressure energy changes into

Manuscript received June 30, 2008; revised December 16, 2008. First published February 6, 2009; current version published April 7, 2009. The Associate Editor coordinating the review process for this paper was Dr. John Sheppard.

M. Lazzaroni and S. Ferrari are with the Department of Information Technologies, University of Milano, 26013 Crema, Italy (e-mail: lazzaroni@dti.unimi.it; ferrari@dti.unimi.it).

L. Cristaldi is with the Dipartimento di Elettrotecnica, Politecnico di Milano, 20133 Milano, Italy (e-mail: loredana.cristaldi@polimi.it).

M. Annoni is with the Dipartimento di Meccanica, Politecnico di Milano, 20133 Milano, Italy (e-mail: massimiliano.annoni@polimi.it).

Color versions of one or more of the figures in this paper are available online at http://ieeexplore.ieee.org.

Digital Object Identifier 10.1109/TIM.2009.2012961

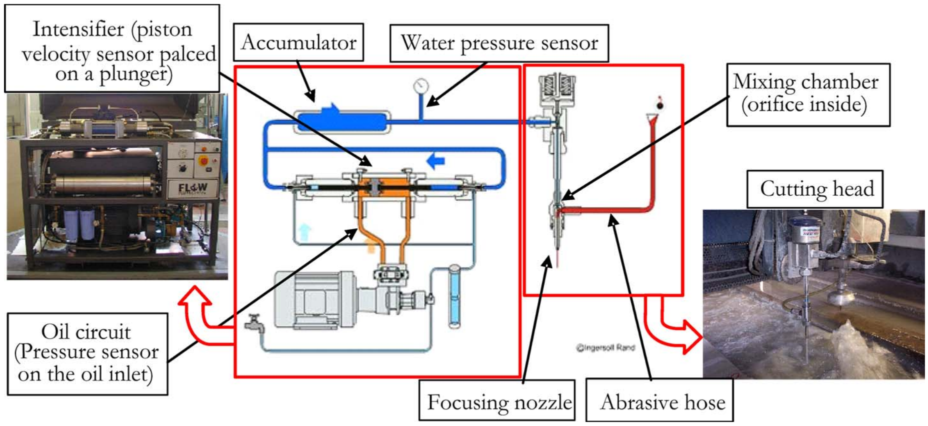


Fig. 1. Main components of the WJ cutting system (scheme in the middle by Ingersoll Rand; photos by Politecnico di Milano).

kinetic energy, and a WJ is formed. Moreover, when an AWJ is considered, solid particles join the water jet inside the mixing chamber. In this particular case, the kinetic energy of abrasive particles is dramatically increased, thanks to the exchange of momentum between water and particles inside the mixing chamber and the focusing nozzle

The AWJ cutting quality typically depends on the process parameter selection (water pressure, abrasive mass flow rate, abrasive granulometry, cutting-head feed rate, and standoff distance), as well as on the fluid-dynamic parameters, such as the orifice and focuser diameters and the mixing-chamber geometry. Aside from the aforementioned parameters, which are considered to be directly valuable variables, some external factors play a nonnegligible role in the cutting quality in terms of roughness and waviness (such as water pressure fluctuation, due to the alternate motion of the pumping system, abrasive mass flow rate fluctuation, workpiece and fixturing system vibrations, and granulometric distribution of the abrasive particles).

A DSP-based system has been designed, realized, and tested to measure the interesting parameters of the complete WJ cutting system such as oil pressure, water pressure, and piston velocity. Furthermore, an analog-to-digital conversion board with simultaneous sampling up to a 200-kHz sampling rate on a single channel with a 16-b resolution has been utilized for electrical motor signal acquisition.

## III. Overview on PR

PR is the scientific discipline dealing with methods for both object description and classification, tasks that are very important in daily life [7]–[9]. Applications of PR techniques are numerous and cover a broad scope of activities, ranging, for example, from satellite-image analysis to biological-signal classification, from traffic analysis and control to biometric recognition, and from seismic analysis to surveillance systems.

The objects to be analyzed and recognized can be signals, images, plain tables of values, or even an ad hoc developed signature evaluated starting from an acquired signal from the field. PR approaches are based on the notion of similarity between two different objects or between an object and a reference object (the target or prototype object). Furthermore, classification is obtained through the object features.

Three concepts are very important in PR: class, pattern, and feature. Classes are categories of objects associated with concepts or prototypes. There is a set of classes that the objects can belong to. For each class, a certain set of representations, named *patterns*, can be used to describe the elements of the class. In this sense, patterns are "physical" representations of the objects. Some of the information contained in each pattern may be redundant or irrelevant for operating the classification task. Features are measurements or attributes derived from the patterns that may be useful for their characterization. The collection of those features that characterize the object of the classification is called the *signature* or *footprint* of the considered object.

As the footprint of an object is generally more simple and compact than the object itself, processing in the feature space is computationally less expensive. Hence, a feature-extraction procedure has to operate on the considered objects. This task is carried out by exploiting the *a priori* knowledge of the object or problem. The feature space has data-driven properties according to the defined similarity measure.

The choice of the features can be based on the domain knowledge given by experts or can be made by using some feature-selection techniques. The deep knowledge of the mechanics and the physics of the particular machinery used may help in choosing well-performing features, but their use may not be generalized to the class of devices.

The aim of assigning an object to a class is a typical example of a classification task. Let us assume that the considered objects can be described through $N$ features. In this case, each object can be represented as a vector

$$\mathbf{x} = [x_1 \quad x_2 \quad \ldots \quad x_N]. \tag{1}$$

For example, if only two features are used during the classification task, the situation can be represented on a plane, as shown in Fig. 2. In general, a feature vector can be represented as a point in the feature space.

The main goal of a classifier is to divide the feature space in regions assigned to classes—the decision regions—or, equivalently, to devise the boundaries between those regions—the decision surfaces. In a multiple-class problem—as the one discussed in this paper—several decision surfaces can be present,

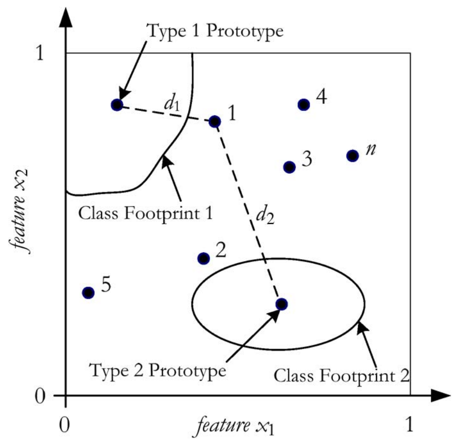


Fig. 2. $f1-f2$ plane. Euclidian distances are also shown on the plane. Classification of object 1 or 2 is a simple task. However, the classification of other points (3, 4, 5, and $n$, for example) is a more complex task.

and arbitrarily complex decision regions can be expected. The configuration of the classifier has to enforce the separation of the classes. It can be obtained through absolute separation, in which case, the features are selected in such a way that each class can be separated from all the others, or through pairwise separation, where the features are selected considering the separation of a pair of classes. This last approach can be used to refine an already-configured classifier, which presents an overlapping pair of classes.

The simple and most-used classification algorithm is the $k$-nearest neighbor ($k$-NN) classifier. The classificatory parameters are simply the collection of the footprints of the data used for its configuration. The classification mechanism is based on a voting scheme. When a signal is presented to the classifier, its footprint is computed, and its distance from all the classifier's footprints is calculated. Then, the new signal is assigned to the class to which the majority of the $k$ footprints that are closer to it belong.

The choice of the $k$ value may be critical, as the optimal value for $k$ grows with both the number of available patterns $n$ and the dimension of the feature space $d$. A proposal was given in [14] where the method is used as a probability-density-function (pdf) estimator. The $k$-NN classifier converges to the Bayesian classifier as $k$ and $n$ grow [15].

In this paper, the diagnostic task and the classification of the working condition of a WJ system are performed by using a black box approach based on soft computing. Soft computing paradigms extract the knowledge by a set of examples of the task that should be performed, while traditional algorithmic paradigms are directly structured by experts. In this paper, the knowledge of an expert of the application is used in the learning process of the proposed tool rather than in the direct recognition of both fault and normal working conditions. The proposed approach is shown in Fig. 3.

## IV. Classification and Diagnostic Tool

In [1], the authors have shown that the load current and instantaneous power signals are strictly correlated to the water pressure values and their behaviors. Any operating conditions

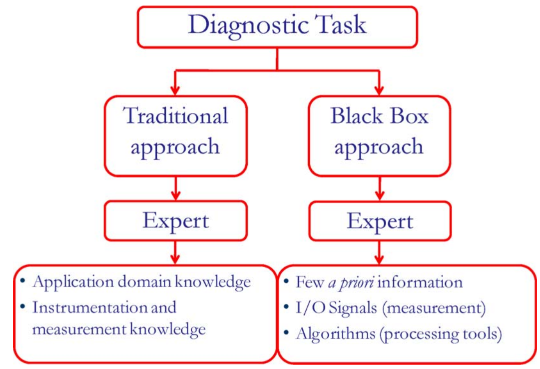


Fig. 3. Two main approaches can be used to perform a diagnostic task. In the traditional approach, experts are directly involved in the design of the solution, while in the black box approach, the knowledge is extracted by a set of examples, which are eventually selected by domain experts.

of the monitored system appear on the main side as a variation in the motor current and instantaneous power. Observing Fig. 4, where these signals are shown, a strict correlation between the modulation of the measured power profile and the motion of the piston can be noted. Moreover, it is possible to observe that the shapes of the power signal depend on the working condition. Signals obviously depend also on the water pressure level and on the changes of the machine status.

From these observations, in [1], the efficiency and effectiveness of the system have been monitored by analyzing the variation of the profiles from the reference condition of the instantaneous power signal.

In this paper, we explored a different method for relating the power signal with the working condition. The proposed method is based on an analysis of the shape of the discrete Fourier transform (DFT) of the power signal [12], [13]. Hence, the characterizing features of the power signal are obtained by a processing operating in the frequency domain. In particular, the features $f_i$ used for the analysis are the first $k$ coefficients of the DFT of the power signal

$$f_i = F(i), \qquad i = 1, \ldots, k \tag{2}$$

where

$$F = \|\mathrm{DFT}(P)\| \tag{3}$$

is the normalized DFT of the instantaneous power signal $P$ (an example of the power signal is shown in Fig. 4).

For each class $j$ identified by the type of orifice, its diameter, and the working pressure, we can define the set of the power signals that belong to this class $D_j = \{P_l | C(P_l) = j\}$ and use the footprint of these signals to compute the class footprint $c_j$ by averaging them

$$c_j(i) = \frac{1}{n_j} \sum_{l=1}^{n_j} F_l(i), \qquad i = 1, \ldots, k \tag{4}$$

where $n_j$ is the number of signals belonging to the $j$th class $n_j = |D_j|$.

The ensemble of the class footprints constitutes a Euclidean classifier. When a new signal has to be classified, its footprint

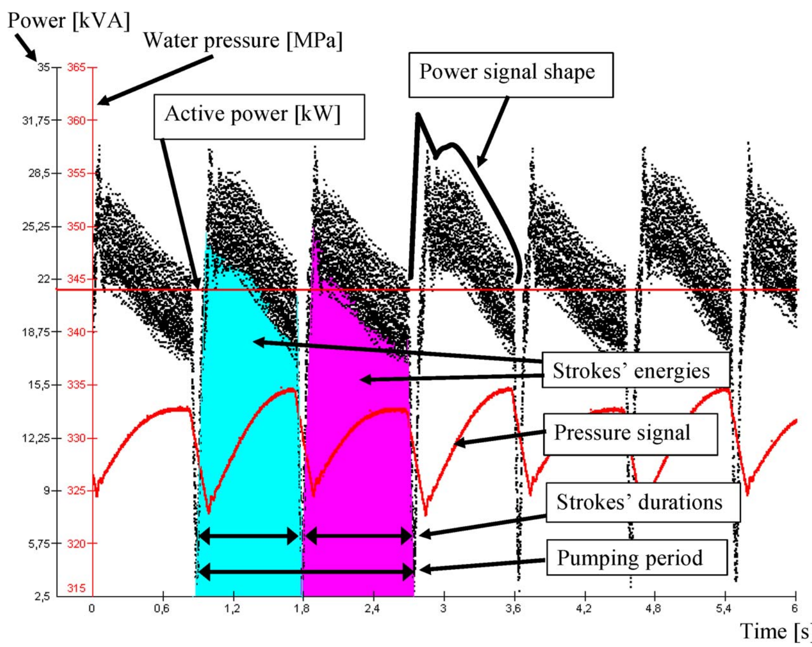


Fig. 4. Reference signals for a specific nozzle. Sampling rate: 3.2 kHz. Sampling period: 6 s.

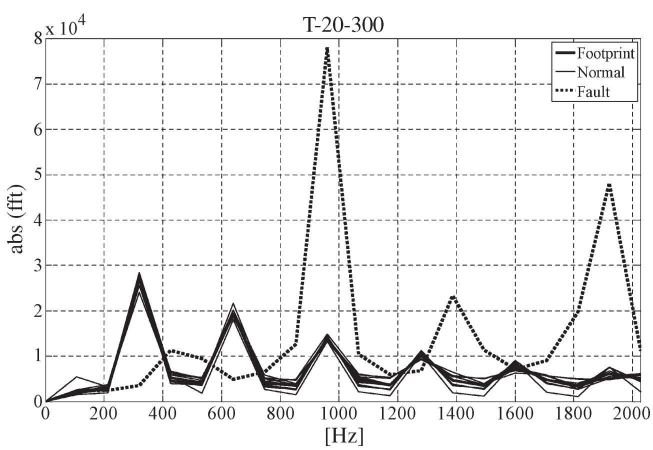


Fig. 5. Feature vector of normal cases, a faulty case, and the footprint of the class. The footprint is represented with the largest line. An example of fault case is represented with dashed line, and finally, non-fault cases are represented with the thin straight line. The non-fault-case footprints are closer to the class footprint than the fault case.

is compared with each class footprint, and the new signal will be assigned to the class whose footprint will be closer to the new signal footprint. Hence, the classification task is realized by using a minimum distance criterion.

As presented in [12], this method leads us to obtain a simple classifier that is able to recognize a faulty condition when the working condition is known *a priori*. This is very clear in Fig. 5, where a footprint coming from a faulty condition is compared with several footprints due to normal working condition.

Two kinds of classification errors may obviously occur in this activity.

Type 1 error: When a signal belonging to a given class $i$ has a footprint that is more similar to the footprint of a different class $j$. It occurs when the classes are overlapped in the feature space and can usually be avoided by using more features (or more meaningful features).

Type 2 error: When a signal belongs to an unknown class. This type of misclassification is harder to cope with. A common approach is to exploit the data used for the configuration of the classifier for obtaining a more accurate description of the region of the space occupied by each class (and considering unknown every signal that falls outside the class regions).

## A. Threshold Classifier

In order to cope with errors of type 2, for each class $j$, we chose to store, in the classifier, not only the class footprint $c_j$ but the mean and the standard deviation of the distance of the class footprint from the signal footprint $\delta_j$ and $\sigma_j$, respectively, as well. This allows the estimation of the region occupied by the $j$th class as the (hyper)sphere centered in $c_j$ having the radius equal to $\delta_j + \lambda\sigma_j$ (for an appropriate value of $\lambda$); when a footprint will result external to each of these spheres, the corresponding signal will be classified as unknown.

In Fig. 6, a simple example related, for the sake of simplicity, to a 2-D case is shown.

Three circles are drawn: a circle having a radius $\delta$ and other two circles having radii of $\delta + \lambda\sigma$, where $\lambda$ is chosen equal to 1 and 2, respectively. As some of the signals of the class are distant from the class footprint for more than the mean distance $\delta$, the region that contains the signals of the class should be described as a sphere that has a radius that is greater than $\delta$. As $\sigma$ describes the variability of the distance with respect to the mean distance $\delta$, it is reasonable to proportionally enlarge the radius of the region to $\sigma$.

Hence, we will consider the region of the domain space occupied by the signal that belongs to the considered class as

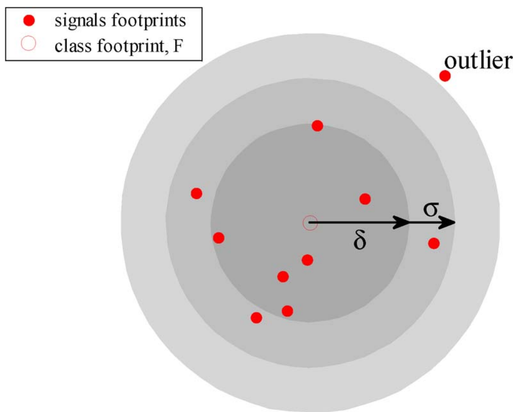


Fig. 6. Using the statistical description of the class for identifying outliers. The footprint of the class is here defined as the barycenter of the footprint of the signals that belong to the considered class. Defining $\delta$ and $\sigma$ as the mean and the standard deviation of the distance of the signal footprints from the class footprint, respectively, the region of the domain that contains the signal of the class can be identified as a sphere centered in the class footprint, having a radius proportional to $\delta$ and $\sigma$. Signals that fall outside this sphere can be considered to be outsiders or signals that belong to a different class.

the sphere centered in the class footprint that has a radius of $\delta + \lambda\sigma$. It should be noted that the class footprint is evaluated by taking into consideration even the outlier that, during the classification task, will not be recognized as part of the class (as its distance from the center is very dissimilar from those of the signal of the class).

### B. Surface Classifier

Observing the signals that refer to the same orifice diameter (see Fig. 7), it is apparent that they share the same pattern warped by an unknown scaling operator that depends on the pressure.

In the frequency domain, this behavior essentially results in a scaling of the frequency components and, hence, in the scaling of the position of the features. Collecting the signals of the same orifice for a continuum of pressure values, it would be possible to observe a drift of the peaks in the feature vectors as the pressure increases. Therefore, it is possible to devise only a class for each orifice, whose footprint incorporates this behavior. The simplest of such footprint will be constituted by a feature surface instead of a feature vector. Such a feature surface can be constructed by distributing the feature signals along the pressure axis, as shown in Fig. 8(a), and by properly interpolating this signal. The feature vectors will act as the skeleton, and a suitable interpolating law will provide the skin. The simpler feature surface can be obtained by linearly interpolating the class signatures [see Fig. 8(b) and (c)].

The points belonging to the resulting feature surface can be described as $S(i,p)$, where the index $i$ refers to the DTF coefficient ($i = 1, \ldots, k$), while $p$ is the value of the working pressure.

For a given pressure $p$, the distance of a sample footprint $s(i)$ (which is a polyline) from the classifier surface $S(i,p)$ (which is a linear mesh) can be defined as a function of the squared distance of the vertices from the surface, as in the following:

$$\mathrm{dist}(s, S; p) = \sum_i (s(i) - S(i,p))^2 . \qquad (5)$$

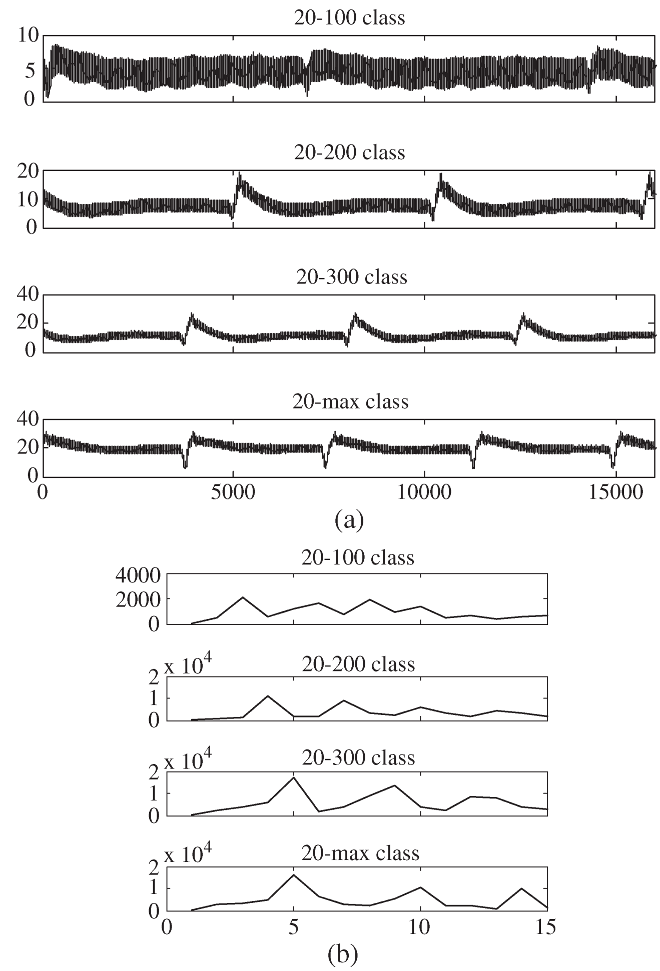


Fig. 7. (a) Samples and (b) the footprints of the same nozzle at different pressures.

The matching pressure $p_{\mathrm{best}}$ for a sample footprint $s$ and a surface $S$ can be defined as the pressure that minimizes the distance between $s$ and $S$

$$p_{\mathrm{best}} = \arg\min_p \sum_i (s(i) - S(i,p))^2 . \qquad (6)$$

This is equivalent to sliding the vector $s$ along the pressure direction and looking for the pressure at which it is most adherent to the surface $S$ (see Fig. 9).

This formulation allows the efficient computation of the best matching pressure by decomposing the optimization problem in (6) in the linear optimization problems given by considering the linear interpolation of two subsequent signatures. In fact, as the surface $S$ has been constructed as a linear interpolation of the set of polylines, each of those characterized by a pressure, the pressure in (6) $p_{\mathrm{best}}$ can be found in two steps. First, the distance between the sample $s$ and the linear interpolation of all the pairs of successive signatures (e.g., the signatures of two successive pressures) are computed. Second, the minimum of these distances is computed, and the pressure at which it occurs is the value of $p_{\mathrm{best}}$. Hence, the computation of the distance of a sample from a signature surface can be reframed as the computation of the distance of the sample from the linear interpolation of two successive signatures.

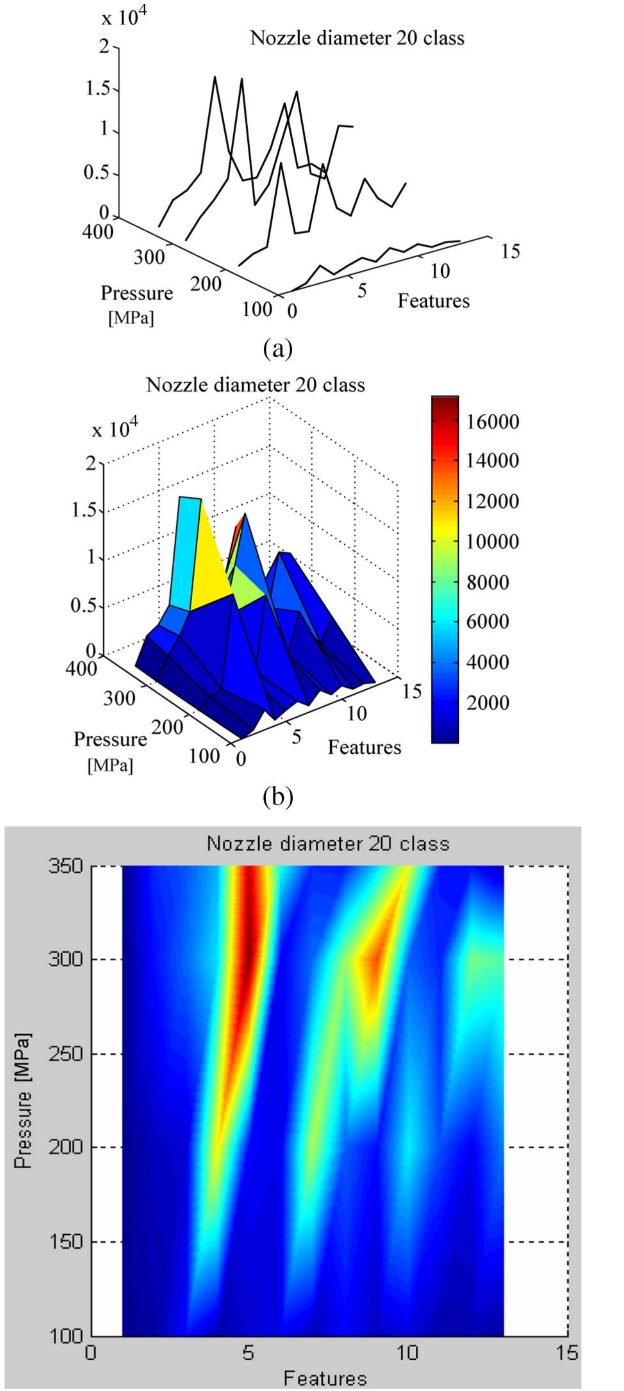


Fig. 8. (a) Skeleton for the proposed feature surface is composed by the feature vectors at the available pressure values. These vectors can be used to build (b) the feature surface by linearly interpolating them. As a result, (c) a pressure-independent footprint of the nozzle is obtained.

Considering two signatures $a$ and $b$ characterized by the pressures $p_a$ and $p_b$, respectively, which are described as $a = [a_1, a_2, \ldots, a_k]$ and $b = [b_1, b_2, \ldots, b_k]$, where $a_i$ and $b_i$ are the vertices of the polylines, in the range $[p_a, p_b]$, the value of the surface $S(i, p)$ is

$$S(i,p) = a_i + \frac{(b_i - a_i)}{(p_b - p_a)}(p - p_a). \tag{7}$$

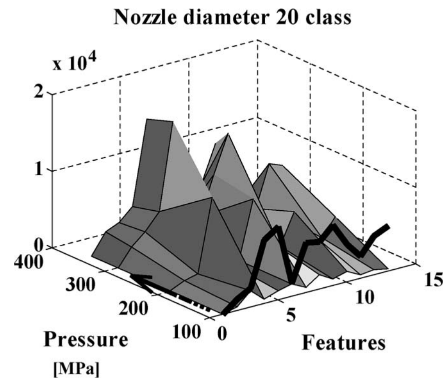


Fig. 9. Graphical representation of the proposed algorithm.

Defining $s_i = s(i)$, the distance between $s$ and $S$ in $[p_a, p_b]$ is

$$\begin{aligned}\mathrm{dist}(s, S; p) &= \sum_i (s_i - S(i,p))^2 \\ &= \sum_i \left(s_i - a_i - \frac{(b_i - a_i)}{(p_b - p_a)}(p - p_a)\right)^2 \\ &= \sum_i (s_i - a_i - d_i(p - p_a))^2 \end{aligned} \tag{8}$$

where $d_i = (b_i - a_i)/(p_b - p_a)$.

The value of $p$ that minimizes the distance in (8) $p_{\text{best}}$ is

$$p_{\text{best}} = \frac{\sum_i d_i(s_i - a_i) + d_i^2 p_a}{\sum_i d_i^2}. \tag{9}$$

Note that, particularly, the feature surface allows the classification of a signal for a known nozzle for an unknown pressure. This feature is very important. In fact, even if a deep experimental activity is mandatory, it is not possible to acquire data from all possible values of pressure. The typical situation in industrial applications is the availability of data at five to ten different working pressures, including the max pressure level.

The ability of the classifier to interpolate the nonavailable situation is mandatory, and it is verified in different case studies, as discussed in the following section.

## V. Experimental Results

The experimental results are obtained by considering many different cases of study. For the sake of simplicity, in this paper, a reduced set of tests is reported.

For this application, we chose $k = 15$, as it allows us to use the most significant coefficients (the performance of the system does not change for a greater value of $k$).

We tested the two kinds of classifiers that were previously described (see Section IV): the single signature (with threshold) classifier and the surface classifier. The data set available for configuring the classifiers is composed of 130 samples of the power signal in ten working conditions: a nozzle with an orifice of two different diameters (0.20 and 0.30 mm) for five different values of working pressure (100, 150, 200, 250, and 300 MPa). The acquisition time for each signal is 9.37 s.

TABLE I
THRESHOLD-CLASSIFIER PERFORMANCE

| | | # signals | # classes | Error |
|---|---|---|---|---|
| **Configuration** | | 130 | 10 | 0.769% |
| **Test** | **known** | 20 | 13 | 5% |
| | **unknown** | 6 | 3 | 0% |

The test set has been composed by two samples for each of the working conditions. Moreover, to test the ability of the single signature classifier to catch unknown working conditions, we added six samples of an orifice made by a different producer, operating in similar working conditions (specifically, 0.20 mm/150 MPa, 0.20 mm/250 MPa, and 0.30 mm/150 MPa).

For the threshold classifier, we choose to experiment on a very conservative setup, setting the parameter $\lambda$ equal to 1. The configuration error of the threshold classifier (i.e., the measure of the misclassification occurred for the configuration data set) has been 0.769% (1/130), stating that a good separation of the classes has been achieved. Furthermore, all the unknown data were correctly classified as unknown, while only one known test sample error has been misclassified (5% test error) as unknown. The results are summarized in Table I.

For the sake of comparison, we challenged a 1-NN classifier with the same test data of the threshold classifier, but without the unknown samples, which the 1-NN classifier is unable to recognize as unknown. The 1-NN classifier performs well, achieving a test error of 0% (with signals only from only known classes).

To test the ability of the surface classifier to recognize patterns that belong to the same orifice but operate in an unknown working condition, we used, for each orifice diameter, only the data related to the 100-, 200-, and 300-MPa values of pressure. Hence, the surface classifier is constituted by two surfaces, which are similar to the one shown in Fig. 9, built by using three subclasses for each surface. Testing the classifier on the configuration data, the surface classifier achieved a configuration error of 1.28% (one error out of 78 signals). The mean error in the pressure prediction has been of 7.60 MPa (with a standard deviation of 11.6 MPa).

The test set has been composed by 20 samples, two for each working condition (including the intermediate pressures of 150 and 250 MPa). Only one of 20 test samples was misclassified (wrong diameter, although the relative error in the pressure estimation has been of 3.57%). The mean absolute error on the pressure estimation has been 8.28 MPa (with a standard deviation of 12.0 MPa). Overall, the error in the pressure estimation for the samples of working conditions directly used in the classifier configuration (i.e., 100, 200, and 300 MPa) has been 4.32 MPa, while for the intermediate working condition, the mean error has been 20.4 MPa (the only misclassification belongs to this subset). The results are summarized in Table II.

## VI. DISCUSSION

The design of the presented classifiers requires one to make some decisions, namely, the choice of the number of features $k$ to be used in the classifiers (for both the classifiers) and the threshold value $\lambda$ for the threshold classifier. Both the design choices have been made by considering the domain knowledge. In general, setting these parameters can be considered to be a problem of model selection, but it is not unusual to exploit the *a priori* information on the problem for enforcing the value of some parameters.

The choice of $\lambda$ should reflect the importance of monitoring an unknown working condition, which is a symptom of a malfunctioning of the system. Small values of $\lambda$ make the classifier sensitive to false unknown classifications, while high values of this parameter increase the probability of classifying an unknown working condition as known. In the experiments that we ran, increasing the value of $\lambda$ to 5, the classifier was able to achieve a test error of 0%. This means that the observed signal was quite distant from the observation belonging to its class.

In the presented applications, the number of features $k$ can be chosen by observing that the signals of the same orifice under different pressure conditions have a similar shape, but scaled, and that the general periodical shape of the signals can be described by the low frequency components of the signal. These considerations allow us to hypothesize that the more informative coefficients of the fast Fourier transform (FFT) of the signals are those relative to the low frequency components. After some preliminary tests, we chose $k = 15$, as the performance of the algorithm does not change sensibly for higher values of this parameter. However, the choice of a higher value for $k$ could be argued, with the motivation that, when more than 15 coefficients of the FFT are used, a more detailed diagnosis would be addressed. However, the following considerations would be taken into account.

1) The goal of this paper is the implementation of a simple method that is able to give a classification of the actual working condition.
2) It is evident that the most important frequency components are concentrated at the low frequencies of the acquired signal (these components carry most of the power of the signal). At these frequencies, which are those close to the piston's frequency, it is possible to extract sufficient information concerning the working condition of the system.
3) The presented approach is intended to be implemented on a very simple microcontroller or microprocessor. In this case, the choice of a small value for the parameter $k$ is mandatory.
4) The use of many FFT coefficients would allow the identification of different spectral lines and how they change with the nozzle diameter and working pressure. However, the experimental activity shows that an appreciable performance of the classifier can be achieved even for low-frequency components.

Aside from the small number of coefficients, the complexity of the algorithm also impacts on the computational resources required by the application. For the proposed classifiers, the computational complexity is linear, and they can therefore be implemented on simple hardware, such as an industrial microcontroller, for example. This is mandatory in case of applications in the industrial environment, where simplicity and

TABLE II
SURFACE-CLASSIFIER PERFORMANCE

| | | #signals | #classes | classification error | pressure error |
|---|---|---|---|---|---|
| Configuration | | 78 | 2 (6 subclasses) | 1.28% | 7.60 MPa |
| Test | known | 12 | 6 | 0% | 4.32 MPa |
| | unknown | 8 | 4 | 12.5% | 20.4 MPa |
| | Overall | 20 | 10 | 5% | 8.28 MPa |

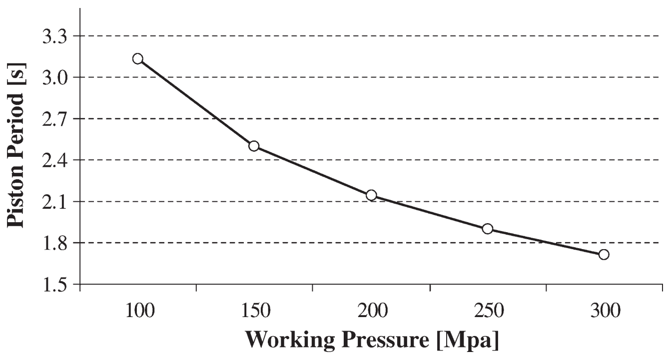


Fig. 10. Relationship between the period of the piston and the provided working pressure. It refers to a 0.3 diameter nozzle, but a similar relationship also holds for the other nozzles.

low cost are very important, even if, in the present case, these constraints are not mandatory.

The main goal of a classifier is to divide the feature space into regions assigned to the classification classes. These regions are called decision regions as aforementioned. If a feature vector falls into a decision region, the associated pattern is assigned to the corresponding class. However, it would be noted that, in many cases, the decision regions are not well separated. This situation leads to the impossibility to perform a correct classification. In our application, this situation is present even in the feature-surface classifier. This classifier, in fact, highlights a misclassification case where a wrong nozzle diameter was recognized. A more detailed examination of the results pointed out that the error (both in classification and in pressure prediction) is not uniformly distributed with respect to the pressure but is higher for low values of pressure (100 and 150 MPa). This fact should be put in relation to the length of the signal acquisition. As shown in Fig. 10, the period of the piston is higher for low pressures; hence, the number of periods acquired is higher for the high values of pressure. Hence, the FFT computation for low pressures is less reliable than for high pressures (where more than one period of the signal has been acquired).

Due to the nature of the applications that the presented classifier should be used in, a few seconds is a very short period of time. The conditions of an orifice (and, in general, of the manufacturing process) will change in a higher order of time (minutes and hours). Therefore, the signals can be acquired for more than a piston period without any impact on the reactivity of the diagnosis system.

Moreover, it is necessary to specify that the feature-surface classifier is mainly used when the nozzle type is known *a priori*. Starting from this point of view, the predicted pressure is a more important performance indicator. Even for the intermediate values of pressure (the unknown cases), the prediction error is less than 10%. It is an accuracy level that is acceptable for the application and is in line with the measurement error of the pressure.

A similar situation happens in security applications, where classification is used for two tasks: identification and verification of users. Identification is the process where the system recognizes the validity of a user's identity, while verification is the process where the system verifies the claimed identity of a user. These two tasks, although very similar, had their own peculiarities, and the same classification system may perform differently for them. In the identification task, the subject under observation is compared with all the known classes. For each class, a matching score is provided, and if there exists any class with an overthreshold score, the subject is assigned to the class with the higher score; otherwise, the subject is classified as unknown. A similar procedure is applied by the threshold classifier. In the authentication task, on the other hand, the subject declares its identity, and the classifier has to estimate the likeness that the subject belongs to the claimed class. This task is similar to those proposed for the use of the surface classifier.

Moreover, the diagnosis case of study differs from the aforementioned security application because the match/nonmatch (or accept/reject) outcome of the classifier can be output after more than one consecutive classification steps. In fact, as the application considered is not critical for the safety of the operators or the machinery and the transition from the optimal working conditions to malfunctioning is very slow, a malfunction can be noticed (and notified) after several samples of the power signal have been classified as overthreshold. Hence, a temporary fluctuation of the measured power signal (as result of transient external causes) should not cause a false malfunction notification.

## VII. CONCLUSION

In this paper, we have shown that the electrical power signal is greatly influenced by the machinery setup and the working conditions. As the measurement of this entity is much more feasible than the direct measurement of the other parameters that influence the working conditions of the system, the exploitation of its relation may lead to an automated method for revealing the machinery state and the presence of (an incoming) faulty behavior.

This fact can suitably be exploited to increase the reliability and availability of the system, thanks to the defined diagnostic algorithm. In particular, two classifiers have been proposed here: a threshold classifier that is able to diagnose known and unknown working conditions and a surface classifier that is able to predict the working pressure of the system.

The simplicity of the proposed approaches leads to the consideration of the possibility of realizing a low-cost real-time diagnostic system. Further developments in this direction are now in progress. Moreover, the surface classifier may be improved by using a more-complex surface-approximating technique.

## REFERENCES


[1] A. Annoni, L. Cristaldi, and M. Lazzaroni, "Measurement and analysis of the signals of a high pressure waterjet pump," in *Proc. IMTC*, Ottawa, ON, Canada, May 16–19, 2005, pp. 1311–1316.

[2] M. Ramulu and M. Tremblay, "Modelling and simulation of pressure fluctuations in high pressure waterjets," in *Proc. 10th Amer. Waterjet Conf.*, 1999. Paper 12.

[3] E. J. Chalmers, "Pressure fluctuation and operating efficiency of intensifiers pumps," in *Proc. 7th Amer. Water Jet Conf.*, Aug. 28–31, 1993, pp. 327–336.

[4] P. J. Singh, "Computer simulation of intensifiers and intensifier systems," in *Proc. 9th Amer. Waterjet Conf.*, 1997, pp. 397–414.

[5] R. N. Tunkel, "Double action hydraulic intensifier," in *Proc. 9th Amer. Waterjet Conf.*, 1997.

[6] M. Annoni and M. Monno, "A model for the simulation of the pressure signal in waterjet systems," in *Proc. 17th Int. Conf. Water Jetting*, 2004, pp. 415–434.

[7] V. Cherkassky and F. Mulier, *Learning from Data*. Hoboken, NJ: Wiley, 1998.

[8] M. Friedman and A. Kandel, *Introduction to Pattern Recognition*. Singapore: World Scientific, 1999.

[9] A. K. Jain, R. P. W. Duin, and J. Mao, "Statistical pattern recognition: A review," *IEEE Trans. Pattern Anal. Mach. Intell.*, vol. 22, no. 1, pp. 4–37, Jan. 2000.

[10] C. Brian, M. Ramulu, and M. Tremblay, "Dynamic modelling and identification of a water jet cutting system," *Math. Comput. Model. Dyn. Syst.*, vol. 9, no. 1, pp. 45–63, Mar. 2003.

[11] L. Cristaldi, M. Lazzaroni, A. Monti, and F. Ponci, "A neuro-fuzzy application for AC motor drives monitoring system," *IEEE Trans. Instrum. Meas.*, vol. 53, no. 4, pp. 1020–1027, Aug. 2004.

[12] M. Annoni, L. Cristaldi, M. Lazzaroni, and S. Ferrari, "Nozzles classification in a high pressure water jet systems," in *Proc. IEEE Instrum. Meas. Technol. Conf.*, May 1–3, 2007, pp. 1–6.

[13] M. Lazzaroni, S. Ferrari, L. Cristaldi, and M. Annoni, "A tool for working condition and nozzles classification for water jet systems," in *Proc. IEEE Int. Instrum. Meas. Technol. Conf.*, May 12–15, 2008, pp. 1435–1440.

[14] K. Fukunanga and L. D. Hostetler, "Optimization of k-nearest neighbor density estimates," *IEEE Trans. Inf. Theory*, vol. IT-19, no. 3, pp. 320–326, May 1973.

[15] T. M. Cover and P. E. Hart, "Nearest neighbor pattern classification," *IEEE Trans. Inf. Theory*, vol. IT-13, no. 1, pp. 21–27, Jan. 1967.


**Massimo Lazzaroni** (S'92–M'92) received the M.Sc. degree in electronic engineering and the Ph.D. degree in electrical engineering from the Politecnico di Milano, Milano, Italy, in 1993 and 1998, respectively.

He is an Associate Professor of electrical and electronic measurements with the Department of Information Technologies, University of Milano, Crema, Italy. His scientific activity includes digital signal processing techniques applied to electrical measurements. In particular, his current research interests are concerned with the application of digital methods to electrical measurements and measurements on electric power systems in nonsinusoidal conditions and the use of soft computing in diagnostic and fault recognition in electrical systems. Furthermore, he is also involved in research activities for the development of industrial sensors and quality control of industrial processes.

Prof. Lazzaroni is a member of the Comitato Elettrotecnico Italiano.

**Stefano Ferrari** (M'09) received the Ph.D. degree in computer engineering from Politecnico di Milano, Milano, Italy, in 2001.

Since 2000, he has been an Assistant Professor with the Department of Information Technologies, University of Milano, Crema, Italy. His research interests are neural networks and soft-computing paradigms and their application to computer graphics, signal processing, and measurement systems.

**Loredana Cristaldi** (S'91–M'01–SM'06) received the M.Sc. degree in electrical engineering from the University of Catania, Catania, Italy, in 1992 and the Ph.D. degree in electrical engineering from the Politecnico di Milano, Milano, Italy, in 1995.

Since 1999, she has been with the Dipartimento di Elettrotecnica, Politecnico di Milano, where she was an Assistant Professor and, since 2005, has been an Associate Professor of electrical and electronic measurements. Her research interests are in the field of the measurement of electric quantities under nonsinusoidal conditions, virtual instruments, and measurement methods for reliability, monitoring, and fault diagnosis.

Dr. Cristaldi is a member of the Italian Association on Industrial Automation and the Italian Group on Electrical and Electronic Measurements.

**Massimiliano Annoni** received the M.Sc. degree in mechanical engineering from the Politecnico di Milano, Milano, Italy, in 1999.

Since 2000, he has been with the Dipartimento di Meccanica, Politecnico di Milano, working in the field of nonconventional machining processes and particularly on water jet technology, where he is involved in research projects and with the activities of the Italian Water Jet Society. Since 2002, he has been an Assistant Professor of manufacturing processes. He is the Editor of the book *Water Jet, a Flexible Technology*, which contains contributions of the main scientists in the field of water jet technology.